

## Novel Hybrid Sensors for Unobtrusive Recording of Human Biopotentials

Robert Matthews  
[robm@quasarusa.com](mailto:robm@quasarusa.com)

Neil J. McDonald  
[neil@quasarusa.com](mailto:neil@quasarusa.com)

Harini Anumula  
[harini@quasarusa.com](mailto:harini@quasarusa.com)

Leonard J. Trejo  
[ltrejo@quasarusa.com](mailto:ltrejo@quasarusa.com)

Quantum Applied Science and Research, 5764 Pacific Center Blvd., #107, San Diego, CA, 92121

### Abstract

*Practical sensing of biopotentials such as EEG or ECG in operational settings has been severely limited by the need for skin preparation and conductive electrolytes at the skin-sensor interface. Another seldom-noted problem has been the need for a conductive connection from the body to ground for cancellation of common-mode noise voltages. At QUASAR, we have developed a novel hybrid (capacitive/conductive) sensor that requires no skin preparation or electrolytes. In addition we have developed a special common-mode follower that allows a dry electrode to be used for the ground. The electronics for the sensors and common-mode follower have low power requirements and are miniaturized to fit within a compact sensor case. We are extending our tests of the hybrid sensor in three human-machine interaction contexts: 1) a real-time system of multimodal physiological gauges for improved human-automation reliability, 2) EEG-based cognitive-overload detection in an urban combat simulation, and 3) a brain-computer interface for EEG-based communication in the severely disabled. In all three contexts we compared the QUASAR hybrid sensors with traditional conductive electrodes for EEG or ECG recordings. We discuss the recording fidelity, noise characteristics, ease of use, and reliability of the hybrid sensors versus the conventional conductive electrodes in all contexts.*

### 1 INTRODUCTION

The increasing complexity and automation of tasks in aerospace and military operations has also increased the need to test, monitor, and maximize human capabilities, both to efficiently use human resources and to enhance personnel performance. In many situations, the exchange of information between computers and their human users is fundamentally limited by human information processing capabilities, and the level of human errors due to reduced alertness, inattention, and cognitive failures occur too frequently with today's complex systems. To meet the increased demands of today's complex systems, DARPA launched the Augmented Cognition (AugCog) program, which aims to use advanced technology to maximize human cognitive capabilities. AugCog is a multidisciplinary approach, which includes research on sensors, biosignal analysis, physiological and behavioral models, algorithms for cognitive state estimation and dynamic computational systems for augmenting cognition and performance.

To estimate human cognitive states, some AugCog systems will use physiological signals such as electrocardiograms (ECG), electrooculograms, (EOG), electromyograms (EMG) and electroencephalograms (EEG). These biosignals have proven to be useful for real-time detection of hazardous states, such as fatigue, inattention, stress, and cognitive overload and for triggering appropriate countermeasures (St. John, Kobus & Morrison, 2003). However, the need to apply obtrusive electrodes to the skin using conductive pastes or gels, often with abrasive skin preparations, has been a serious barrier to deployment. To solve this "sensor problem" the AugCog program has supported research on novel biosensors which provide high quality biosignals while also being comfortable and easy to use. To be truly unobtrusive, these biosensors should be donned or doffed quickly by the wearer, require no skin preparation, produce no skin irritation, and be worn comfortably for extended periods.

The measurements described herein were made using QUASAR sensors and are applicable to three operational contexts: a) a real-time system of multimodal physiological gauges for improved human-automation reliability, b) EEG-based cognitive-overload detection in an urban combat simulation, and c) a brain-computer interface for EEG-based communication in the severely disabled. In all three contexts we compared the QUASAR hybrid sensors with traditional conductive electrodes for EEG or ECG recordings. These contexts are relevant because QUASAR is performing collaborative research with DoD, academic, and clinical partners in these areas. At the Florida Institute for Human and Machine Cognition we are performing research on multimodal physiological gauges for improved human-automation reliability in the context of unmanned aerial vehicle control tasks. At The Scripps Research Institute, we are studying the effects of cognitive overload on EEG and ECG measures in the context of an urban combat simulation. At the Wadsworth Institute we are cooperating with efforts to develop unobtrusive biosensors for use in EEG-

based brain-computer interfaces for the severely disabled (Wolpaw & McFarland, 1991), but which also may find applications in future human-computer interfaces (Trejo *et al.*, 2003; Trejo, Matthews & Rosipal, 2006). We will report on simultaneous tests of QUASAR biosensors side-by-side with conventional “wet” electrodes in laboratory tasks designed to produce the effects observed in these three contexts. These include variations in EEG rhythms such as theta and alpha bands or spectral patterns, amplitude effects in event-related potential (ERP) components such as the P300, changes in heart-rate or heart-rate variability, and eye-blinks or eye movements estimated with the EOG. Our focus was on limited tests to permit qualitative and semi-quantitative comparisons of QUASAR biosensors with conventional electrodes. As such, the present sample sizes do not permit statistical comparisons. Finally, we will discuss the recording fidelity, noise characteristics, ease of use, and reliability of the hybrid sensors versus the conventional conductive electrodes in all contexts.

## 2 METHODS

### 2.1 QUASAR Capacitive Biosensors

QUASAR has recently developed novel capacitive biosensors (Fig. 1), which meet the AugCog requirements for operational recordings of ECG, EOG, and EMG signals. The QUASAR sensors couple to the electric fields of the body *capacitively*, requiring no skin contact and no skin preparation. Detection of human bioelectric signals using purely capacitive coupling (Fig. 1a) was first developed in 1967 (Richardson, 1968) and patented in 1970 (Richardson & Lopex, 1970). Unlike prior methods, QUASAR’s capacitive biosensors (Fig. 1b) can tolerate very small capacitances to the source, which enables the new electrodes to be operated at a standoff from the skin – up to 1 cm in practice (Matthews, McDonald, Fridman, *et al.*, 2005). This spacing makes the new technology relatively immune to lift-off from the body. At millimeter separations,  $Z_s$  is approximately given by the standard expression for a parallel plate capacitor, and is thus inversely proportional to the spacing between the electrode and the body. For prior capacitive electrodes that require skin contact, this dependence is so sensitive that if the electrode moves from touching the surface of the skin to just 100  $\mu\text{m}$  away,  $Z_s$  changes by approximately a factor of 10. This susceptibility to displacement means traditional capacitive (insulated) bioelectrodes must be held tightly against the skin and, as a result, they are little different in terms of operational use from conventional resistive contact electrodes. However, for the new QUASAR electrodes, spacing from the body of only 1 mm means that a 100  $\mu\text{m}$  increase in stand-off changes the capacitance by only 10%, and by only 1% at 1 cm. This property allows implementation of a truly wearable system. In the experiments described here, QUASAR biosensors were used to measure ECG, EOG, and as reference electrodes for EEG.

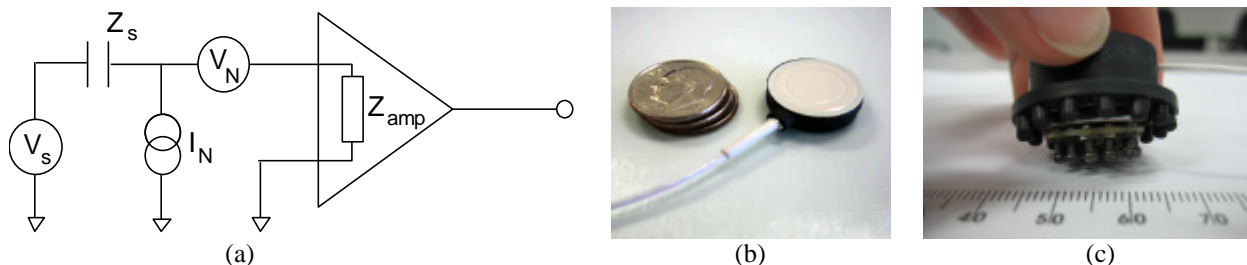


Figure 1. (a) Circuit for a capacitive electrode connected to an amplifier.  $V_s$  is the potential at the electrode,  $Z_s$  is the electrode impedance (pure capacitance),  $V_N$  and  $I_N$  are the voltage and current noise respectively of the amplifier, and  $Z_{amp}$  is the amplifier input impedance; (b) QUASAR capacitive biosensor; (c) QUASAR hybrid EEG biosensor.

### 2.2 QUASAR Hybrid EEG Biosensors

The QUASAR capacitive biosensors used for ECG, EMG, and EOG will also measure EEG from relatively hair free skin, such as on the forehead. However, operational measurement of EEG requires application through considerable thicknesses of hair. To meet this requirement, QUASAR has developed a novel *hybrid biosensor* (Fig. 1c), which enables through-hair measurements of EEG without any skin preparation. In contrast to conventional EEG electrode technology, which relies on a low impedance contact to the scalp, hybrid biosensors use a combination of high impedance resistive and capacitive contact to the scalp, and innovative processing electronics to reduce pickup and susceptibility to common-mode signals on the body (Matthews *et al.*, 2005). The hybrid biosensor consists of an

electrode, an ultra-high input impedance amplifier circuit, and ancillary electronics that include a gain/filter module (GFM), a common-mode follower (CMF) and a data acquisition/communications module (DACM).

The hybrid biosensor contacts the skin with a set of ‘fingers,’ each of which is small enough to reach through hair without trapping hair beneath the finger (thereby preventing electrical contact to the scalp). As the contact impedance between the scalp and each finger can be as high  $10^7 \Omega$ , the amplifier electronics are shielded and placed as close as possible to the electrode in order to limit interference caused by the pickup of external signals. Power for the biosensors is supplied by the GFM, which also provides signal conditioning and anti-aliasing of the measured EEG signals. The GFM can be configured to provide individual EEG signals or high common-mode rejection ratio difference signals (CMRR  $\sim 100\text{dB}$ ) between biosensors.

The CMF is a proprietary technology used to reduce the sensitivity of the hybrid biosensor to common mode signals on the body. The CMF is a separate hybrid biosensor (not necessarily on the scalp) that measures the potential of the body relative to the ground of the amplifier system. An ultra-high input impedance for the CMF ( $\sim 10^{12} \Omega$ ) ensures that the output of the CMF tracks the body-ground potential with a high degree of accuracy. The CMF output is used in the GFM as a reference for the EEG measurement by the electrodes. In this way, the common-mode signal appearing on the body is dynamically removed from the EEG measurement. This typically achieves a CMRR of 50 to 70 dB. In the experiments described here, QUASAR Hybrid EEG Biosensors were used to measure EEG at three active recording sites: Fz, Cz, and  $C_3$  (Jasper, 1958).

### 2.3 Data Acquisition

During these experiments we recorded six channels of EEG (electroencephalogram), one vertical EOG (electrooculogram) and one ECG (electrocardiogram) channel. The six EEG channels simultaneously recorded EEG from three QUASAR hybrid biosensors and conventional three wet electrodes measured at three sites (Fig. 2a): Cz, Fz and  $C_3$  locations. The wet electrodes were positioned 2 cm anterior to the hybrid electrodes, which were themselves positioned at the nominal Cz, Fz and  $C_3$  locations. Preparation of the scalp for the wet electrodes included abrasion with Nu-Prep, followed by cleaning with alcohol and then application of Grass EC2 electrode paste. No preparation of the scalp was performed at the sites for the QUASAR electrodes.

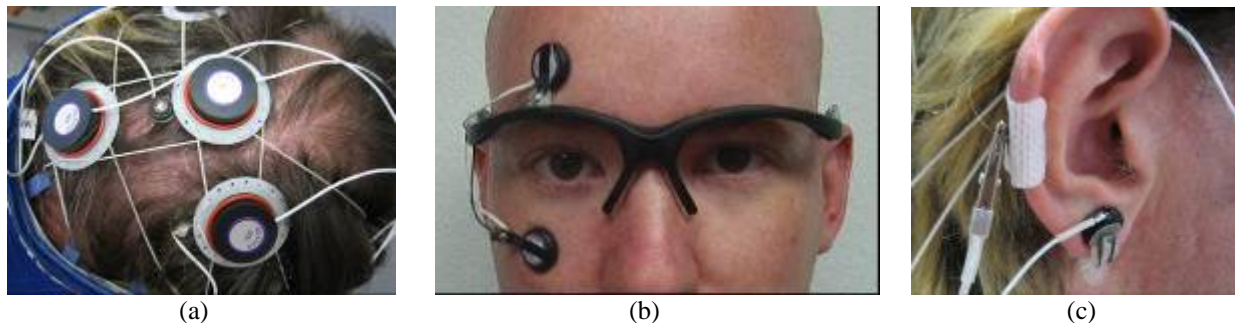


Figure 2. Location of sensors for (a) EEG measurements, (b) EOG measurements, (c) CMF.

The vertical EOG measurement was made about the right eye using QUASAR capacitive bioelectrodes integrated into a pair of glasses (Fig. 2b). ECG measurements were made using QUASAR capacitive bioelectrodes integrated into a belt positioned about the subject's torso. The electrodes were positioned just below the pectoral muscles, aligned with the subject's nipples.

Independent grounds were used for the wet and hybrid electrodes. The ground reference for the wet EEG electrodes was a standard pre-gelled disposable Ag-AgCl electrode placed upon a prepared site on the mid-posterior aspect of the subject's right pinna (Fig. 2c). The electrical ground for the EEG and EOG electrodes was a high impedance ground through the cap. The electrical ground for the QUASAR ECG electrodes was a high impedance ground through the belt. No preparation of the skin was performed to improve the contact impedance of either high impedance ground. The high impedance grounds were connected to the ground of the data acquisition system. The CMF for EEG and EOG measurements for QUASAR electrodes was placed on the right earlobe (Fig. 2c). The CMF for the ECG measurements was placed adjacent to the ground of the belt.

The data acquisition system was a National Instruments NI-4472 PCI (24-bit, 8 channel delta-sigma) card installed in a desktop computer running a LabView-based data acquisition application. Anti-aliasing of the data was not necessary before digitization because of the details of the sigma-delta data acquisition. Signals were sampled at 12 kHz, then digitally filtered with a 300 Hz (-3dB) low-pass anti-alias filter before the samples were decimated to a sample rate of 1200 Hz. Each signal was corrected for the intrinsic gain in the sensors and ancillary electronics (EEG channels – gain=20, EOG channel – gain=100, ECG channel – gain=100). Signals were displayed in real time for monitoring purposes and saved on the hard disk drive for later analysis.

The subject (male, 37 y) was seated in a comfortable chair positioned approximately 1 m from a laptop computer (15" screen) that displayed information during the course of the measurements. Measurements were made in the laboratory at QUASAR's San Diego facilities. The area immediately adjacent to the experiment was cordoned off to prevent interference due to people moving nearby, but activity continued in the rest of the laboratory as usual. No shielding of the subject was attempted.

## 2.4 Tasks

The subject performed the following sequence of tasks:

### 2.4.1 *Eyes Open/Closed (desynchronization of EEG alpha rhythm)*

Recording of EEG with a subject at rest with eyes open or closed is part of a standard clinical EEG test. A prominent feature of the eyes-closed EEG is a pronounced alpha rhythm, which disappears (or desynchronizes) when the eyes are opened. To measure this effect, we recorded EEG while the subject looked at a fixation point on the laptop screen (an 'X' in the center of the screen) for a period of 30 seconds. This was repeated with the subject's eyes closed. Both measurements were then repeated. A single cycle of eyes open/eyes closed measurements was repeated at the conclusion of the P300 session (see below).

### 2.4.2 *Real and Imaginary Button-press (desynchronization of EEG $\mu$ -Rhythm)*

One approach for brain-computer interfaces involves volitional control of  $\mu$ -rhythm, an EEG oscillation in the 10 Hz range recorded over motor cortex, such as at site C<sub>3</sub>. To obtain EEG comparable to that of a  $\mu$ -rhythm BCI situation we recorded EEG during a button-press task and an imaginary button-press task (Trejo *et al.*, 2003; Trejo, Matthews & Rosipal, 2006). The subject then looked at the fixation point for a period of 30 seconds, performing a discrete movement every 5 seconds for a period of 60 seconds. (In this case the movement was clicking the mouse button on the laptop.) The subject rested briefly before repeating the discrete movement task. Then the subject performed an imaginary button click every 5 seconds for a period of 60 seconds. The subject rested briefly before repeating the imaginary button click task. The fixation/discrete movement/imaginary steps were then repeated.

### 2.4.3 *Memory/Cognition Measurements (modulation of EEG alpha and theta rhythms)*

Memory load and mental arithmetic are frequently used to control mental workload, and produce distinct effects on EEG spectra, including modulation of theta (4-7 Hz) and alpha (8-12 Hz) bands (Gevins *et al.*, 1998; Wallerius, Trejo, Matthews, Rosipal & Caldwell, 2005). Such effects are key features used by real-time algorithms to monitor human cognition during decision-making and control tasks such as the UAV task being studied at IHMC and the combat simulation task being studied at TSRI (Trejo *et al.*, 2006; Wilson & Russell, 2003). The subject looked at the fixation point for a period of 30 seconds while counting down from 100 in steps of 2. This is defined as the easy task. Then the subject looked at the fixation point for a period of 30 seconds while counting down from 100 in steps of 7 (hard task). These tasks were then repeated.

### 2.4.4 *Visual Oddball Task (modulation of P300 ERP component)*

An array of alphanumeric characters was displayed on the laptop screen. At intervals of 0.6 seconds either a row (Fig. 3a) or a column (Fig. 3b) would be randomly highlighted, with the constraint that 84% of the events were column intensifications and 16% were row intensifications. These correspond to standard and deviant stimuli respectively. For these measurements the ECG channel was replaced with an audio signal associated with each stimulus that was output by the laptop: a tone (standard) or a click (deviant) for stimulus synchronization. The audio signal was not audible by the subject. Data were collected while the subject counted the number of deviant signals for a period of 300 seconds. The display was run continuously for this period. After a 1 minute rest, the test was repeated.

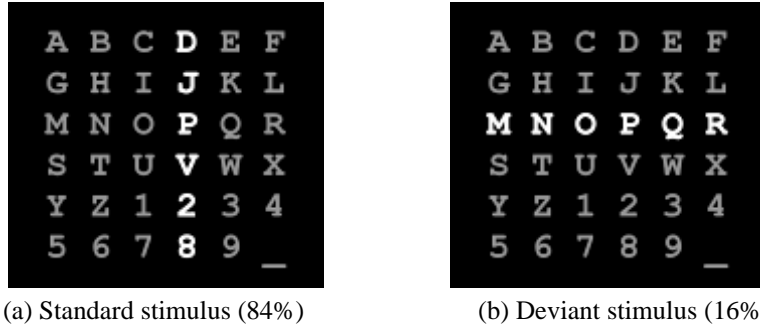


Figure 3. Sample images of (a) standard and (b) deviant stimuli for the visual oddball task.

### 3 RESULTS

#### 3.1 Sample Recordings and Inter-sensor Correlations

A representative segment of normalized time series recordings from all data channels in the second eyes-open EEG task appears in Fig. 4. Although only a single 30-s segment is shown, the recording quality was consistent over the entire experiment without obvious changes in signal quality or noise levels. To focus our comparisons on the signals of interest we low-pass filtered and decimated time series of each EEG channel to a new sampling rate of 100 Hz, or an effective bandwidth of 0-40 Hz. Any linear trend in the time series of each channel was also removed.

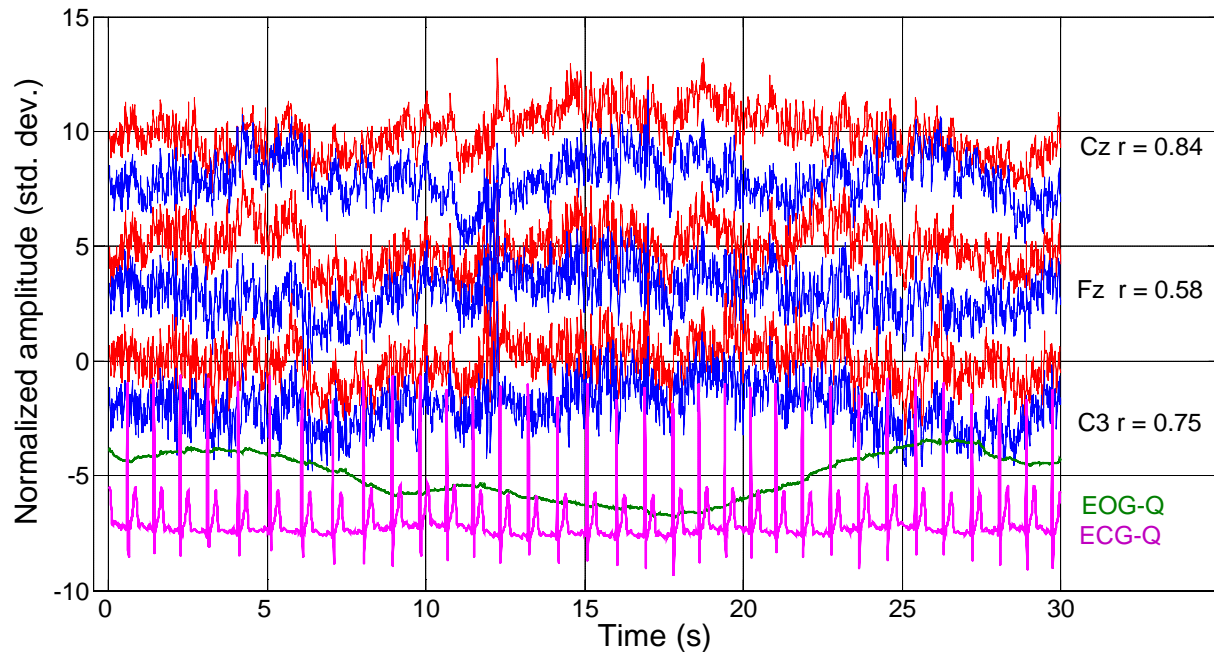


Figure 4. Representative recordings of all channels from the second eyes-open EEG task. All signals have been normalized to zero mean and unit standard deviation. Signals have been displaced vertically to allow comparisons. From the top down, the traces are for sensors: QUASAR Cz, wet Cz, QUASAR Fz, wet Fz, QUASAR C<sub>3</sub>, wet C<sub>3</sub>, EOG, and ECG. Red and blue lines are for the QUASAR sensor and wet electrode recordings, respectively.

The correlation coefficients for the QUASAR-wet sensor time-series for the electrode pairs at Cz, Fz, and C<sub>3</sub> were 0.8436, 0.5814, and 0.7498, respectively. For comparison, in the filtered recordings the interchannel correlations of the wet sensors ranged from 0.81 to 0.87 and for the QUASAR sensors from 0.60 to 0.71. The EOG and ECG recordings were unremarkable, with consistently low noise and high stability over all sessions. Some of these correlations are misleading because there still remain short segments of uncorrelated artifacts or baseline shifts in the time series. When the correlations over a series of 1-s segments for the worst-case pair (QUASAR Fz – wet Fz) were examined, 26/30 correlations had values of 0.80 or higher (Fig. 5).

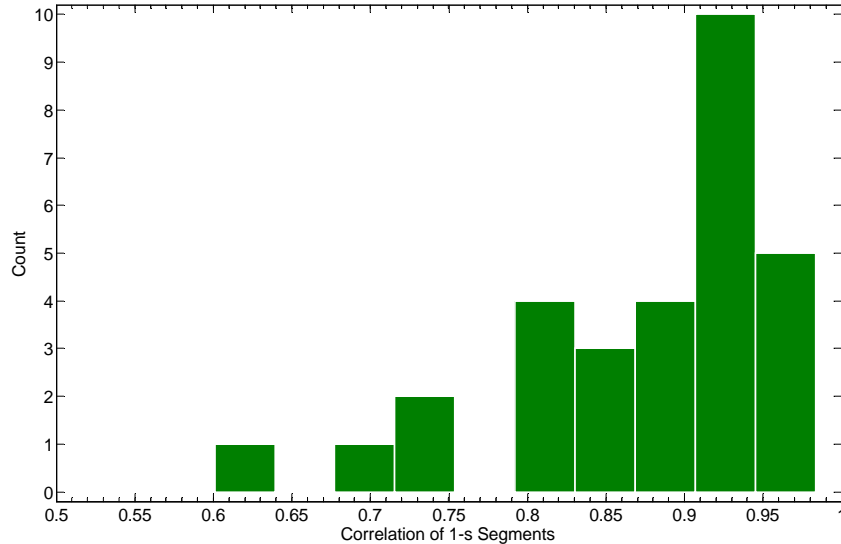


Figure 5. Histogram of Pearson correlations over a series of consecutive 30 1-s segments for QUASAR Fz - wet Fz. In 26/30 segments the QUASAR-wet correlation was 0.80 or higher. The correlation coefficient for the two sensors over the entire 30-s series was 0.5814. EEG signals band-limited to 0-40 Hz.

### 3.2 Eyes-open / Eyes-closed EEG Task.

The power spectral density (PSD) functions of the EEG signals for QUASAR and wet sensors were similar across eyes-open and eyes-closed tasks, with both sensors detecting the desynchronization of the alpha rhythm when the eyes were open (Fig. 6). The beta rhythm (15-25 Hz) also desynchronized when the eyes were open. PSDs were computed using Welch's method from the decimated (100 Hz) EEG with window length = 2 s, overlap = 1 s and FFT length = 1024. In the eyes-closed session, the inter-sensor Pearson product-moment correlation coefficients of the PSDs for QUASAR-wet sensor pairs at Cz, Fz, and C<sub>3</sub> were 0.9979, 0.9632, and 0.9979, respectively. In the eyes-open session, the inter-sensor Pearson correlation coefficients of the PSDs for QUASAR-wet sensor pairs at Cz, Fz, and C<sub>3</sub> were 0.9922, 0.9929, and 0.9981, respectively. For these PSDs, we take a conservative estimate of the number of independent frequency bins as 50, or about 1/10 of the number of FFT points. Using this estimate, any correlation with a value greater than 0.4267 is significant (one-tailed  $t(1,48) = 3.269, p < .001$ ).

### 3.3 Real and Imaginary Button-press task.

The power spectral density (PSD) functions of the EEG signals for QUASAR and wet sensors were highly similar across button-press and imaginary button-press tasks. Fig. 7 presents PSD data for the QUASAR electrodes. Both sensor types detected an increase in power of the alpha rhythm when the subject pressed the button as compared to resting/eyes-open or imaginary button-pressing. Being somewhat speculative, we see that both sensor types also show a peak near 12 Hz in the eyes open condition that was absent in the imaginary condition and indistinct from the alpha rhythm in the button-press condition. Since the C<sub>3</sub> electrode is above the central motor area of cortex, this 12 Hz peak could indicate synchronized  $\mu$ -rhythm during resting/eyes-open and which desynchronized during real or imaginary button pressing. Such  $\mu$ -rhythm desynchronization is one of several methods that subjects may learn to control EEG-based brain-computer interfaces. However, these results are not clear enough to warrant a strong inference of  $\mu$ -rhythm. Additionally, there was an anomalously high peak in the theta band near 6 Hz for the button press task. This peak is unexpected, and was not considered further as it is not usually regarded as being important for brain-computer interface tasks. As for the eyes-open/closed conditions, PSDs were computed using Welch's method from the decimated (100 Hz) EEG with window length = 2 s, overlap = 1 s and FFT length = 1024. In the button-press condition, the inter-sensor Pearson correlation coefficients of the PSDs for QUASAR-wet sensor pairs at Cz, Fz, and C<sub>3</sub> were 0.9994, 0.9985, and 0.9985, respectively. In the eyes-open session, the inter-sensor Pearson correlation coefficients of the PSDs for QUASAR-wet sensor pairs at Cz, Fz, and C<sub>3</sub> were 0.9950, 0.9984, and 0.9941, respectively.

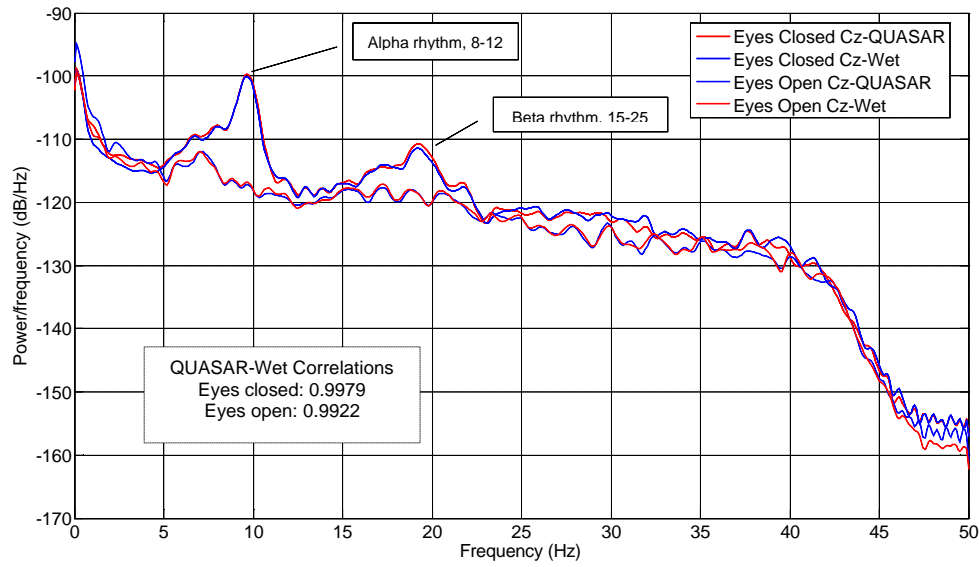


Figure 6. Power spectral density functions of 30-s EEG recordings during the second eyes-closed session and the following eyes-open session. PSDs were computed using Welch's method from the decimated EEG with parameters of window length = 2 s, overlap = 1 s, FFT length = 1024, and sampling rate = 100 Hz.

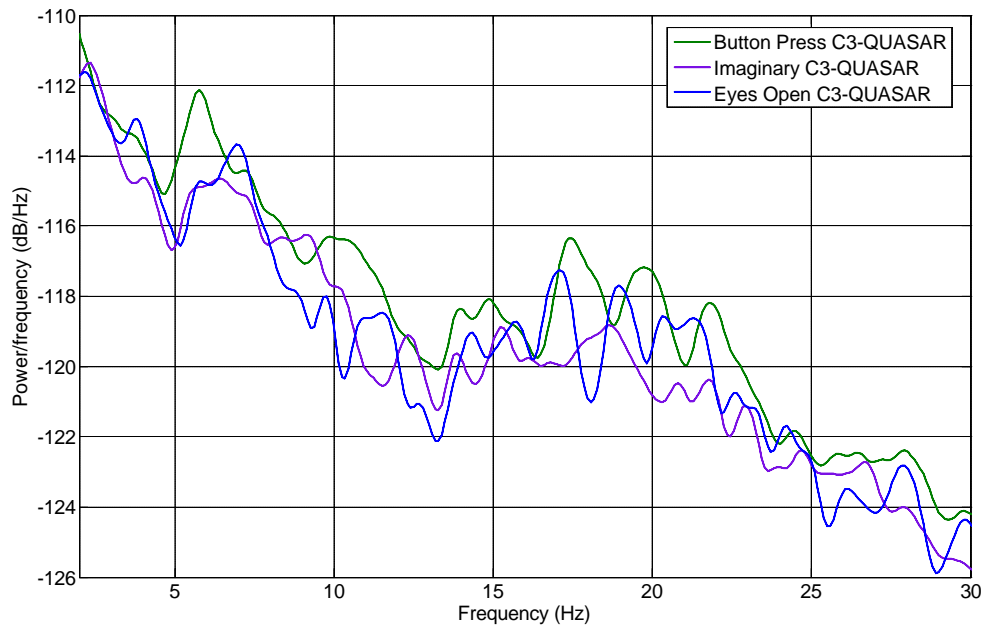


Figure 7. Power spectral density functions of 60-s EEG recordings during the second button-press task, second imaginary button-press task and the eyes-open session (30-s) immediately before the button-press task. PSDs were computed using Welch's method from the decimated EEG with parameters of window length = 2 s, overlap = 1 s, FFT length = 1024, and sampling rate = 100 Hz. (a) QUASAR EEG sensors. (b) Wet EEG sensors.

### 3.4 Memory / Cognition Task

The power spectral density (PSD) functions of the EEG signals for QUASAR and wet sensors were highly similar across the two levels of the memory/cognition tasks. Both sensors types detected increases in theta band power (5-7 Hz) and lower alpha band power (8-9 Hz) when the subject counted backward in steps of seven as compared to steps of two (Fig. 8). Similarly, both sensor types also indicated a mid- and high alpha band peaks near 10 Hz and

12 Hz in the easy condition which were absent or greatly reduced in the hard condition. This behavior agrees with that reported elsewhere (Gevins *et al.*, 1998). Power was also greater in the range of 14.5 to 16.5 Hz in the easy condition than in the hard condition. Peaks near 15 Hz are often referred to as sensorimotor rhythm, or SMR.

It was found that the EEG amplitudes for the hard task exceeded those for the easy condition by factors of 2.1 and 1.6 at 7 Hz (theta) and 9 Hz (low alpha) respectively. As compared to the hard condition, EEG amplitudes for the mid-alpha (10 Hz) high alpha (12 Hz) and SMR (15 Hz) peaks were greater in the easy condition than in the hard condition by factors of 1.73, 1.85, and 1.60 respectively. Based on distance from the SMR source, EEG amplitude in the SMR band may be higher at  $C_3$ , which is above the sensorimotor strip of cortex, than at Cz, which is farther away. However, no difference in SMR amplitude was evident between Cz and  $C_3$ . Nevertheless, the SMR effect was considerably greater at  $C_3$  than Cz, where EEG amplitude was greater by a factor of 2.83 at 15 Hz in the easy condition than in the hard condition.

As for other conditions, PSDs were computed using Welch's method from the decimated (100 Hz) EEG with window length = 2 s, overlap = 1 s and FFT length = 1024. In the easy condition, the inter-sensor Pearson correlation coefficients of the PSDs for QUASAR-wet sensor pairs at Cz, Fz, and  $C_3$  were 0.9993, 0.9960, and 0.9854, respectively. In the hard condition, the inter-sensor Pearson correlation coefficients of the PSDs for QUASAR-wet sensor pairs at Cz, Fz, and  $C_3$  were 0.9987, 0.9495, and 0.9941, respectively.

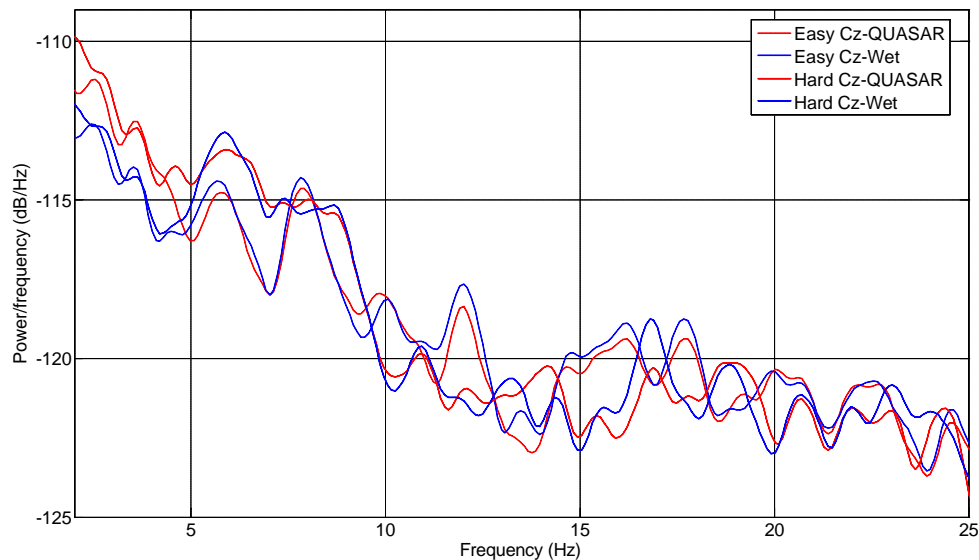


Figure 8. Power spectral density functions of 30-s EEG recordings during the second easy and hard levels of the memory/cognition task. Easy-hard spectral differences appear in the theta (4-7), alpha (8-12), and SMR (14-16 Hz) bands of the EEG spectrum. Inter-sensor correlations between QUASAR and wet sensors at Cz in the easy and hard conditions were 0.9993 and 0.9987, respectively.

### 3.5 P300 Oddball Task

Average ERPs for sessions 1 and 2 of the P300 task were first computed separately and compared. Analysis of the P300 task data involved averaging epochs consisting of samples from -100 ms to +500 ms relative to the stimulus onset separately for standard and deviant stimuli for each replication of the P300 task. Accuracy of stimulus timing for each epoch was performed using the audio channel from the first frame of each video stimulus in the video. There were 432 standards and 83 deviants for Run 1 and 430 standards and 84 deviants for Run 2. No rejection was performed for recording artifacts. However, the averages were subsequently corrected for EOG artifacts using a linear regression estimate of the average EOG artifact at each EEG electrode.

Visual inspection revealed similar waveforms and component effects, so the two sessions were averaged to improve the ERP signal to noise ratio (Fig. 9). EOG artifacts substantially distorted the average ERP for the standard stimuli and to a lesser degree, the averages of the deviant stimuli. After artifact removal, clear differences between the ERP averages for standard and deviant stimuli were evident. In particular, both the QUASAR and wet sensors indicated

a large P300 component with a peak latency of about 400 ms in the deviant averages which was not present in the standard averages. At Cz and C<sub>3</sub> the P300 waveforms for both sensor types were similar, indicating a peak amplitude of about 40  $\mu\text{V}$ . At Fz, the QUASAR sensor measured a P300 amplitude of 50  $\mu\text{V}$ , over 20  $\mu\text{V}$  larger than that of the wet sensor. Both sensor types appear to exhibit enough sensitivity to visual P300, as needed for the detection of stimulus intensifications used for P300-based BCI systems.

### 3.6 ECG and EOG Measures

The primary feature of ECG used in mental state estimation is the heart rate (HR) and its variability (HRV), which both require accurate measures of heart beat timing. Our present results indicate that QUASAR capacitive sensors record accurate ECG with high signal to noise ratio (Fig. 4) as needed for real-time heart-rate measurements. The present ECG recordings serve to reconfirm separate tests using QUASAR capacitive sensors reported elsewhere (Matthews *et al.*, 2005), where QUASAR electrodes achieved a 99.8% correct classification of the heart rate.

Similarly, previous QUASAR research has shown that EOG recordings with QUASAR capacitive biosensors are reliable and of high quality (Matthews *et al.*, 2005). The primary features of EOG signals used in mental state estimation and human-computer interfaces are waveforms corresponding to blinks and eye movements. These waveforms serve to correct EOG artifacts in EEG recordings and may also provide blink- and eye-movement related measures, such as blink amplitude, duration, and frequency or timing of saccades. In our present experiments our focus was on control of EOG artifact, which corrupted EEG recordings with blink- and eye-movement related artifact at both QUASAR and wet sensor sites. Correction of artifacts was not performed in the EEG-related tasks, but was performed in the P300 task, as needed for improvement of ERP signal to noise ratios (Fig. 9).

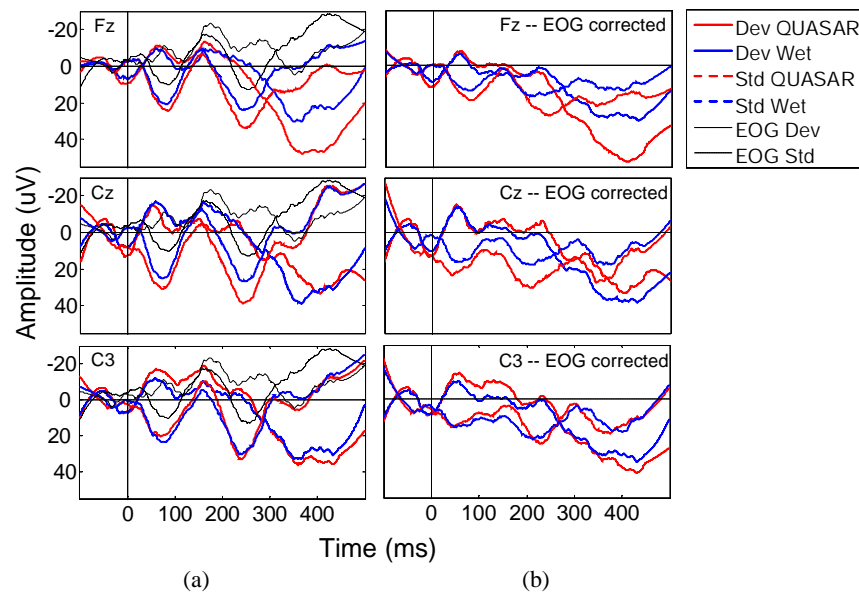


Figure 9. P300 ERP waveforms averaged across P300 task sessions at locations Fz, Cz, and C<sub>3</sub>. (a) Averages without EOG artifact correction. (b) Averages following EOG artifact correction. Positive is plotted downwards.

## 4 DISCUSSION

Although the present experiments were limited to one subject, the quality and consistency of the recordings and the effects we measured show that capacitive and hybrid QUASAR biosensors function as well as conventional “wet” sensors in the following three human-computer interaction contexts: 1) a real-time system of multimodal physiological gauges for improved human-automation reliability, 2) EEG-based cognitive-overload detection in an urban combat simulation, and 3) a brain-computer interface for EEG-based communication in the severely disabled. While the present experiments did not fully replicate these contexts, the critical measurements required to apply biosensors in these contexts were replicated with adequate fidelity.

For real-time systems and human-computer interfaces, ongoing research at QUASAR, IHMC, TSRI, and the Wadsworth Institute is producing sensors and algorithms which signal the onset of adverse or hazardous mental states such as fatigue or cognitive overload and the timing of control signals such as EEG desynchronization or P300

ERPs. The key measures being used in this research include EEG, ERP, ECG, EOG, visual gaze and pupil size. Only the first four of these require biosensors, as the other two are measured optically. Of these, however, only the EEG and ERP measures require careful analysis, for the following two reasons: we have already shown in other work that ECG recordings produced by QUASAR biosensors are highly accurate and reliable, and the recordings of EOG signals with QUASAR biosensors are also reliable and of high quality, and can serve for artifact correction of EEG signals acquired using both QUASAR and wet sensors (Matthews *et al.*, 2005). The EEG recordings are the critical signals, for which additional evidence is required for application to human-computer interfaces.

Our results provide clear and convincing evidence of EEG signals which correlate extremely well with simultaneously recorded wet electrodes. Correlations of such signals in the time domain were typically at 0.8 or better, when DC drift or out-of-band frequencies, including 60-Hz noise, were excluded by filtering. In the spectral domain, the PSD functions of QUASAR and wet EEG recordings within the EEG band of 0-40 Hz were remarkably high, typically above 0.99.

Besides showing that the signals of interest are correlated across sensor types, sensitivity to the effects typically used for human-computer interaction – namely modulation of EEG rhythms, such as alpha, theta, and SMR, and the detection of P300 ERPs for discrete stimuli – is also required for operational sensor use. Our results show that each of these effects is clearly visible in recordings made with QUASAR biosensors and conventional wet electrodes.

Future research is required on comfortable mounting systems for QUASAR biosensors, additional noise immunity for operational environments, and mobile electronics for battery-powered operation and wireless data transmission. We are currently performing research and development in each of these areas at the QUASAR laboratory and in the laboratories of our partner organizations.

## 5 ACKNOWLEDGEMENT

The authors would like to thank our collaborators for their useful contributions during the planning of the experiments described in this paper: Anil Raj (Institute for Human and Machine Cognition, Pensacola, FL), John Polich (The Scripps Research Institute, La Jolla, CA), and Jonathan Wolpaw, Dennis McFarland and Theresa Vaughan (The Wadsworth Institute, Albany, NY).

## 6 REFERENCES

- Gevens, A., Smith, M.E., Leong, H., McEvoy, L., Whitfield, S., Du, R., et al. (1998). Monitoring working memory load during computer-based tasks with EEG pattern recognition methods. *Human Factors*, 40: 79-91.
- Jasper, H. H. (1958). The ten-twenty electrode system of the international federation, *Electroencephalogr. Clin. Neurophysiol.* 10: 371-375.
- Matthews, R., McDonald, N.J., Fridman, I., Hervieux, P. & Nielsen, T. (2005). The invisible electrode – zero prep time, ultra low capacitive sensing. 11th International Conference on Human Computer Interaction (HCII), Las Vegas, NV, 22-27 July, 2005.
- Richardson, P.C. (1968). The insulated electrode: A pasteless electrocardiographic technique, *Proc. Annu. Conf. Eng. Med. Biol.* 9:15-7.
- Richardson, P.C. & Lopez, A. Jr. (1970). Electrocardiographic and bioelectric capacitive electrode, U.S. Patent 3,500,823.
- St. John, M., Kobus, D. A., & Morrison, J. G. (2003, December). DARPA Augmented Cognition Technical Integration Experiment (TIE). Technical Report 1905, SPAWAR Systems Center, San Diego.
- Trejo, L.J., Kochavi, R., Kubitz, K., Montgomery, L. D., Rosipal, R., & Matthews, B. (2006, January). EEG-based estimation of mental fatigue. Manuscript submitted for publication. Available on-line at : <http://www.oaic.net/ltrejo/publications/Submission-Proof-EEG-based-estimation-of-mental-fatigue.pdf>.
- Trejo, L.J., Matthews, B., & Rosipal, R. (2006). Brain-computer interfaces for 1-D and 2-D cursor control: designs using volitional control of the EEG spectrum or steady-state visual evoked potentials" that appeared in *IEEE Trans Neural Syst Rehabil Eng.*,14(2): 225-229.
- Trejo, L.J., Wheeler, K.R., Jorgensen, C.C., Rosipal, R., Clanton, S., Matthews, B., Hibbs, A.D., Matthews, R., & Krupka, M. (2003). Multimodal neuroelectric interface development, *IEEE Trans. Neural Sys. Rehab. Eng.*, 11(2): 199-204.
- Wallerius, J., Trejo, L. J, Matthews, R., Rosipal, R., and Caldwell, J. A. (2005). Robust feature extraction and classification of EEG spectra for real-time classification of cognitive state. 11th International Conference on Human Computer Interaction (HCII), Las Vegas, NV, 22-27 July, 2005.
- Wilson, G.F., & Russell, C.A. (2003). Real-time assessment of mental workload using psychophysiological measures and artificial neural networks. *Human Factors*, 45(4): 635-643.
- Wolpaw, J. R. & McFarland, D. J. (1991). An EEG-based brain-computer interface for cursor Control, *Electroenceph. Clin. Neurophysiol.*, 78: 252-259.